Efficient management of industrial electric vehicles by means of static and dynamic wireless power transfer systems

The International Journal of Advanced Manufacturing Technology
https://doi.org/10.1007/s00170-022-10216-0

ORIGINAL ARTICLE

Efficient management of industrial electric vehicles by means of static and dynamic wireless power transfer systems

Alberto Faveto[1] · Luigi Panza[1] · Giulia Bruno[1] · Vincenzo Cirimele[2,3] · Saverio Stefano Furio[3] · Franco Lombardi[1]

Received: 7 June 2022 / Accepted: 27 September 2022

Abstract
Industrial companies are moving toward the electrification of equipment and processes, in line with the broader energy transition taking place across the economy. Particularly, the energy efficiency and, consequently, the reduction of environmental pollution of intralogistics activities have become a competitive element and are now an actual research and development objective. A wireless power transfer is a contactless electrical energy transmission technology based on the magnetic coupling between coils installable under the ground level and a coil mounted under the vehicle floor, and it represents an excellent solution to decrease the demand for batteries by reducing vehicle downtimes during the recharge. This work aims to define a methodology to determine the optimal positioning of wireless charging units across the warehouse, both for static and dynamic recharging. To this aim, firstly, a mathematical model of the warehouse is proposed to describe transfers and storage/retrieval operations executed by the forklifts. Then, an integer linear programming problem is applied to find the best possible layout of the charging infrastructures. The optimal solution respects the energetic requirements given by the customer and minimizes the overall system cost. The proposed approach was applied to optimize the installation in a real-size warehouse of a tire manufacturing company. Several scenarios were computer generated through discrete event simulation in order to test the optimizer in different warehouse conditions. The obtained results show that integrated dynamic and static WPT systems ensure a constant state of charge of the electric vehicles during their operations.

Keywords Electric vehicles · Battery charging · Wireless power transfer · Green warehouse · Integer linear programming · Discrete event simulation

✉ Alberto Faveto
alberto.faveto@polito.it

Luigi Panza
luigi.panza@polito.it

Giulia Bruno
giulia.bruno@polito.it

Vincenzo Cirimele
vincenzo.cirimele@unibo.it

Saverio Stefano Furio
saveriostefano.furio@enermovesrl.it

Franco Lombardi
franco.lombardi@polito.it

[1] Department of Management and Production Engineering, Politecnico di Torino, Corso Duca degli Abruzzi 24, 10129 Torino, Italy

[2] Department of Electrical, Electronic, and Information Engineering, Università di Bologna, Cesena Campus, 47521 Cesena, Italy

[3] Enermove s.r.l, 10129 Corso Castelfidardo 30/ATorino, Italy

1 Introduction

Regulators and corporate policies are more and more pointing attention to climate issues and energy sustainability. For instance, in Europe, the objective is to cut domestic greenhouse gas emissions by at least 80% by 2050 compared to 1990 [1]. These concerns have led to the rapid growth of electric vehicles (EVs) due to their ability to reduce pollution and gas emissions and save fuel costs [2, 3].

The rapid development of new technologies and applications to develop the EV automotive field has generated idea spillovers and directed innovation in other sectors where electric engines were already well established, e.g., indoor material handling or airport electric ground support equipment. Vehicles have to be electrically powered to reduce pollutant emissions and guarantee breathable air and workers' safety in these applications. However, the electrification of a large number of vehicles triggers several issues due

Published online: 12 October 2022

to the environmental impact and sustainability of batteries. The batteries of electric vehicles need to be recharged quite frequently and require considerable time to reach the desired state of charge. In order to reduce the charging frequency, the capacity of the battery has to be increased. In this case, the battery pack volume raises, which leads to a proportional and substantial increase in the vehicle's weight with a consequent boost in energy consumption per unit of distance traveled [4]. In order to reduce the charging time, the battery swap procedure can be exploited [5, 6]. However, this technique requires a more extensive stock of batteries, higher than $n + nR$, where n is the total number of vehicles in service and R is the ratio between the average charging time and the average discharging time. In this case, the impact of the battery life cycle is quite significant since the efficient recycling of batteries at the end of their life is not consolidated [5, 7].

Among others, a promising technology for battery charging is the wireless power transfer (WPT), a contactless electrical energy transmission system. It is based on the magnetic coupling between coils installed under the ground level, called the transmitters, and a coil mounted under the vehicle floor, called the receiver [8]. In WPT, the transmitter and receiver are independent, and the recharge process can start automatically when the vehicle is over the transmitter. Moreover, the problem of electrical erosion and deposition of dust, dirt, and chemicals is avoided thanks to the absence of contact and the embedding in the vehicle, which allows the system to have a longer life cycle and less need for intervention and maintenance [8]. For all these reasons, this study aims to propose a model to evaluate the best deployment of a combined static and dynamic WPT charging system within a warehouse to achieve a required level of charge while minimizing plant costs. SWPT systems can be placed in dedicated areas where the vehicles stop and can be recharged, e.g., parking slots and docks. At the same time, DWPT systems can be used to create a charging lane constituted by multiple transmitting coils placed below plant pavement. These coils automatically activate when the forklift is over them [9, 10]. The system allows charging the vehicle continuously, eliminating the charging breaks typical of the battery swap method. Moreover, the power needed for this application is similar to the slow charging of batteries. So, it does not require any electrical system improvement, which typically must be realized during the installation of fast charging systems.

The paper is organized as follows. Section 2 presents the literature review available on the topic. Section 3 defines the methodology for installing a WPT system in a warehouse. Firstly, a statistical discretization of the warehouse is performed, then an integer linear programming (ILP) model is applied to evaluate the best positioning of coils inside the plant in order to satisfy project constraints while minimizing the cost. In Sect. 4, the proposed methodology is applied to a real case study, i.e., a warehouse used as a distribution center by a tire manufacturing company in Europe, while in Sect. 5, the results of the application are described. Finally, Sect. 6 presents some conclusions and future works.

2 State of the Art

In literature, two types of WPT technologies are defined based on the maximum allowed distance between the transmitter and the receiver: radiative (far-field) WPT and non-radiative (near-field) WPT. The former is concerned about energy transfer at long distances since an antenna transmits the energy to a receiver via electromagnetic waves [11]. The latter concerns the transmission of energy at short distances, and it is based on the near-field magnetic coupling of coils [12]. In this work, we focused on the near-field WPT. For what concerns the applications devoted to the charge of electric vehicles, the near-field WPT can be indicated as static WPT (SWPT) or dynamic WPT (DWPT) [13, 14]. SWPT applies to vehicles stopped or parked during the charge, while DWPT is able to supply power to the vehicle while it continues to move. A general scheme of the main components of a WPT system applied to a forklift is depicted in Fig. 1. The system comprises a transmitter pad (i.e., transmitter coil and auxiliary parts), mounted under the floor level, and a receiver pad mounted onboard the vehicle. The AC voltage of the warehouse electric grid is converted to a stable DC voltage through a power factor corrector (PFC) AC/DC converter. Downstream the AC/DC converter, each transmitter is powered via a DC/AC converter giving rise to the variable magnetic field responsible for the wireless power transmission. Finally, onboard the forklift, the AC voltage at the output of the receiver pad is converted again into DC signal to charge the vehicle battery.

WPT involves the use of electromagnetic fields at frequencies that typically range from 10 to 100 kHz in the presence of relevant air gaps between the coils. This is why the assessment of human exposure to the electromagnetic field must be appropriately taken into account during both the design stage of the WPT system and in the management of system operations. In [15], it is possible to find an assessment for the automotive application of a 20-kW DWPT system. As they highlight, the system is safer and compliant with the guidelines if the coil receiver is placed at the center of the vehicle, i.e., in a position in which both transmitter and receiver coil can be adequately shielded. DWPT has not yet found much use in the automotive industry, even though research in this field is making great strides. In literature, it is possible to find several works demonstrating technical feasibility [16–18]. Nevertheless, according to the literature,

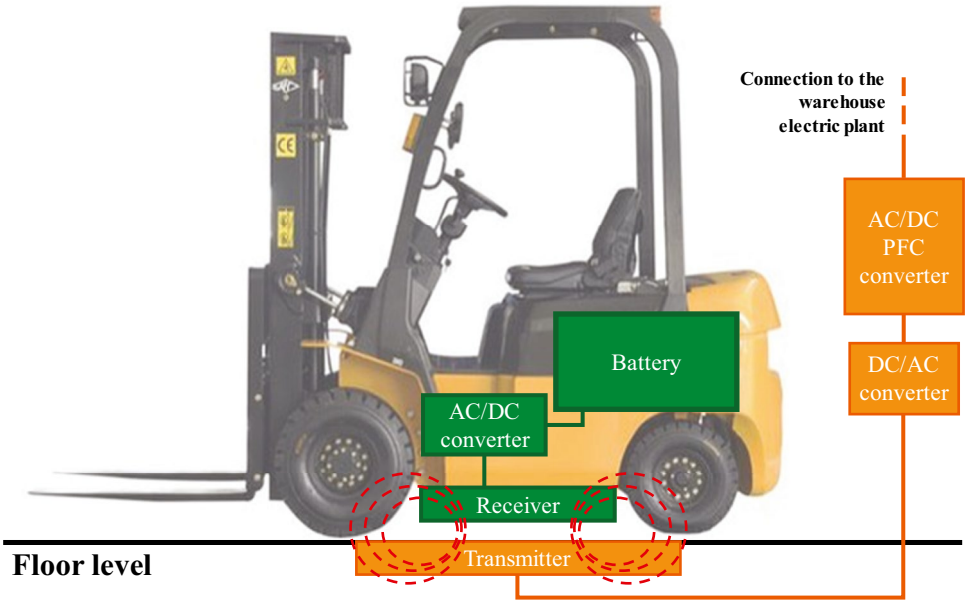

Fig. 1 Scheme of the main components of a (static) WPT system. In the dynamic version, the DC/AC converter and the transmitter (in orange) are replicated to build a charging lane

the use of WPT could find fertile ground in indoor mobility, particularly for industrial warehouse vehicles [19, 20].

In fact, according to the lean management perspective, the time spent in the warehouse has no added value; however, stocks are necessary for many reasons (anticipating demand, decoupling processes, buffer production, etc.). Furthermore, the time spent in the warehouse generates additional holding costs, i.e., the daily cost of maintaining the product in the warehouse in terms of energy consumption, overhead, and the risk of perishability and obsolescence of the products [21]. For all these reasons, a green approach to warehouse management is increasing in importance, and it has been the subject of research studies. In recent years, the term green warehouse has been defined, i.e., as a new management approach to minimize energy consumption and emissions in the holding and handling of warehouse stock [22]. On the other hand, an economic and social management perspective is well established in literature by means of the concept of lean warehouse [23]. To the extent of a more sustainable warehouse from an economic, environmental, and social perspective, performance measurement is shifting to a more comprehensive outlook, assessing the pollutant emissions, energy saving, but also the condition of workers and the ergonomics of the most frustrating tasks [21, 24].

Several works have focused on optimizing WPT infrastructure through a mathematical modelization, e.g., in [25], the authors developed a model to find the optimal location of DWPT facilities and design the optimal battery sizes of electric buses and electric public services with multiple lines. While in [26], a methodology is proposed to find the optimal location of a wireless charging system for buses on the airport apron. Finally, [27] and [28] study a model to evaluate wireless transfer technology in vehicular traffic. To the best of our knowledge, no researcher has addressed the problem of WPT system allocation and optimization in warehouses or other indoor applications. We think this technology could be appealing in an indoor application, and in this paragraph, we present some reasons.

Warehouse forklifts usually employ two kinds of batteries:

- The most used type is valve-regulated lead-acid batteries (VLAB). They are employed due to their low cost and their high reliability. However, lead-acid batteries present some downsides, such as low energy density (35 –50 Wh/kg) and high weight. Although EVs' battery weight represents a drawback, for what concerns the electric forklifts, the weight is not a significant issue because it is used as a counterweight inside them, helping maintain the center of gravity during operational lifts. [29–31].
- Lithium-ion batteries are the most modern solution. They are lighter and present superior energy density (114–125 Wh/kg), a longer life cycle, and greater efficiency. However, they are still not widely adopted as, on the counterpart, they are more expensive [30, 31].

One of the most diffused methods to execute the recharge consists of the battery swap procedure [5, 32]. The exhausted battery is substituted with a charged one. Though, this operation requires skilled personnel and introduces many safety risks [32]. It is possible to use a single battery that should be frequently partially charged using a particular power supply, providing a current up to three times higher than the nominal charging one. However, the drawback of this solution is

represented by the high number of breaks needed for frequently charging the battery and, as aforementioned, the more significant number of battery stock required. On the other hand, thanks to DWPT, it is possible to create a charging lane constituted by multiple transmitting coils placed below plant pavement. These coils activate automatically when the forklift passes over. This system allows to continuously charge the vehicle by keeping a constant state of charge and eliminating the charging breaks typical of the battery swap method. Moreover, the power needed for this application is similar to the one for the slow charging of batteries, and so it does not require any electrical system improvement, which typically must be realized during the installation of fast charging [33].

As aforementioned, DWPT can potentially solve the trade-off between battery autonomy and charging time. In a DWPT system, the batteries can have a smaller capacity and therefore be cheaper. Besides, as there is no need to stop vehicles for recharging, the total number of forklifts (and batteries) can be lower in indoor applications like plants or warehouses. Both of these advantages mean that the system has a lower environmental impact. Fewer vehicle breaks and greater utilization of batteries can drive a service life intensification. In our opinion, this phenomenon can have an extraordinary effect on warehouse sustainability because a small number of resources are needed and operate more efficiently. Additionally, this sustainable approach positively affects warehouse economic performances: fewer pauses mean greater productivity, and fewer resources mean a minor use of the company's funds.

3 Methodology

The proposed methodology for the WPT system installation in a warehouse is composed of four phases.

The first phase is the mathematical definition of the warehouse. The warehouse is modeled as an undirected graph by using nodes and edges placed on the discretized working area. All the operations carried out by the electric forklifts must be defined, as well as the definition of the DWPT system to be installed.

The second phase is the probabilistic assessment of the forklift positions, which is carried out based on the time spent by the forklifts in the different working zones during a working shift. Such computation has a twofold purpose: on the one hand, the time distribution of the forklifts represents the criterion by which the optimization algorithm computes the whole WPT system layout, including both SWPT and DWPT systems. On the other hand, the knowledge of each temporal contribution relating to the different service phases, which are the travel time in unloaded conditions, the operational time in the storage/retrieval point, the travel time in loaded conditions, the operational time in the docking area, and the waiting time in the docking area allow the assessment of the energy demand in a working shift.

The third phase is the energetic analysis in order to compute the state of charge (SoC) variation of the forklifts after a working shift. It includes the energy spent by the forklifts during their different service phases, as well as the energy absorbed due to charging systems by means of WPT. The SoC variation is a customer requirement, so the WPT system layout must be able to guarantee the residual energy required by the customer at the end of the working shift.

The fourth phase is the formulation of the optimization problem. The output of the optimization problem is the computation of the WPT system displacement layout that allows the fulfillment of the problem constraints, the satisfaction of the SoC requirement, and the cost minimization of the system.

The present work takes as a reference for the WPT systems the data provided by Enermove s.r.l. (http://www.enermove.com/), an Italian company partner of this work. In the upcoming sections, all the phases of the methodology are described in detail.

3.1 Warehouse modeling

In this phase, in order to design a mathematical model of the warehouse, the following items are defined: (i) warehouse map, (ii) DWPT, and (iii) forklift operations. These three elements and their definitions are exhaustively detailed in the three subsequent subparagraphs.

3.1.1 Warehouse map model

A warehouse can be defined as a set of corridors, i.e., paths along with the forklifts move to store items in the racks or retrieve items from them. Each corridor has an orientation: if it is parallel to the x-axis, it is called a horizontal corridor; otherwise, it is a vertical corridor. For instance, in the warehouse depicted in Fig. 2, three corridors are present, two vertical and one horizontal.

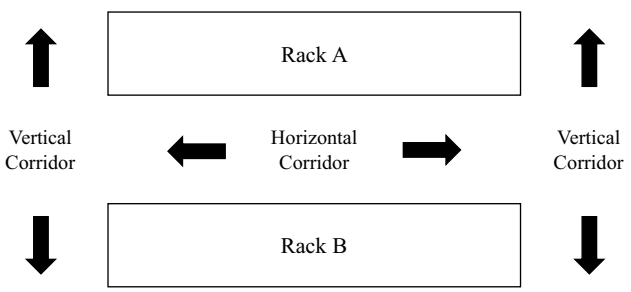

Fig. 2 Warehouse with three corridors

It is possible to define $\mathscr{H}$ the set of all the horizontal corridors in the warehouse, and $|\mathcal{H}| = H$ its cardinality. In a similar way, $\mathscr{V}$ is the set of all the vertical corridors in the warehouse, and $|\mathcal{V}| = V$ its cardinality.

$$\mathcal{H} = \{1, 2, \dots, H\} \tag{1}$$

$$\mathcal{V} = \{1, 2, \dots, V\} \tag{2}$$

In order to discretize each warehouse corridor, it is possible to define a set $\mathcal{N}$ of warehousing nodes with cardinality $|\mathcal{N}| = N$, equal to the number of all the nodes within the discretized warehouse, excluded the entry dock ones:

$$\mathcal{N} = \{1, 2, \dots, N\} \tag{3}$$

The corridors are discretized into smaller areas using warehousing nodes. Any point of the aisle that the forklift can traverse is associated with a node if that node is the closest to that. In this way, we reduce the warehouse into a simple graph of nodes and edges. All the events that happen in a bidimensional warehouse area are associated with the single closest unidimensional node.

Each warehousing node belongs to one of the following categories, as shown in Fig. 3:

1. *Horizontal node*: a node belonging to a horizontal corridor, where a DWPT module can be installed just along the x direction;
2. *Vertical node*: a node belonging to a vertical corridor, where a DWPT module can be installed just along the y direction;
3. *Cross nodes*: a node belonging to both a horizontal and a vertical corridor, where a DWPT module can be installed in both directions;
4. *Impossible node*: a node where no DWPT module can be installed because, in that area, it is not possible to insert a coil.

For each warehousing node i, the following properties are defined:

- n_i: a sequential integer number starting from 1 representing the node identifier.
- $(x_i,\ y_i)$: the Cartesian coordinates of the node in accordance with the chosen reference system.
- $cat_i \in \{1, 2, 3, 4\}$: the category of the node.
- $horc_i \in \mathcal{H} \cup \{0\}$: the horizontal corridor to which the node belongs to (0 otherwise).
- $verc_i \in \mathcal{V} \cup \{0\}$: the vertical corridor to which the node belongs to (0 otherwise).
- $onf_i \in \{0, 1\}$: the operational node flag with value 1 if an operation of storage or retrieval can be executed in the node, 0 if it is only a passing node.

Each couple of adjacent nodes is connected by a non-oriented edge, and DWPT modules can be placed only across the defined edges. As all the nodes within the warehouse map are equally spaced, all the edges have the same length, and since a DWPT module developed by Enermove has a length of 2.5 m, we have decided on an edge length of 0.5 m as a trade-off between the flexibility of DWPT module placement and graph complexity. In a similar way, as done for the warehousing nodes, it is possible to define a set of edges $\mathscr{E}$ with cardinality $|\mathcal{E}| = E$.

$$\mathcal{E} = \{1, 2, \dots, E\} \tag{4}$$

Each edge $e \in \mathcal{E}$ is identified by an edge ID e_e: a sequential integer number starting from 1.

An additional element to fully represent the warehouse is the docking node, defined as the closest node to the docking area. The docking node has the same properties as the warehousing nodes, but no DWPT module can be placed on it; thus, all docking nodes belong to the 4th category. The docking areas deal with the loading and unloading operations of the items from the truck. We have defined a set of docks Δ with cardinality $|\Delta| = D$:

$$\Delta = \{1, 2, \dots, D\} \tag{5}$$

Each dock $j \in \Delta$ is identified by the following parameters:

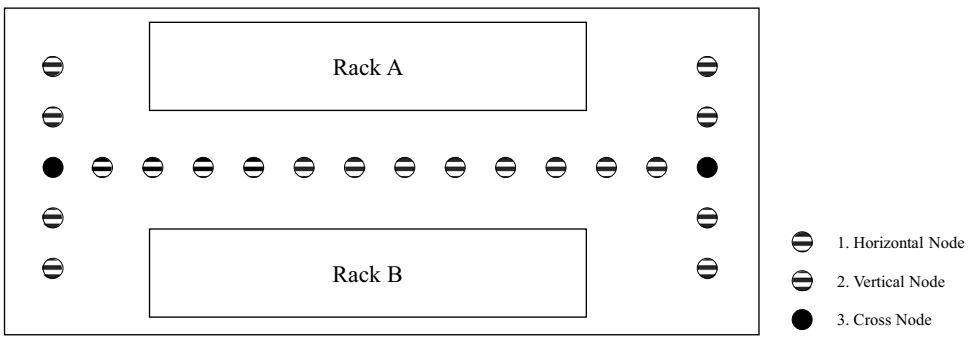

Fig. 3 Warehouse representation with node categories

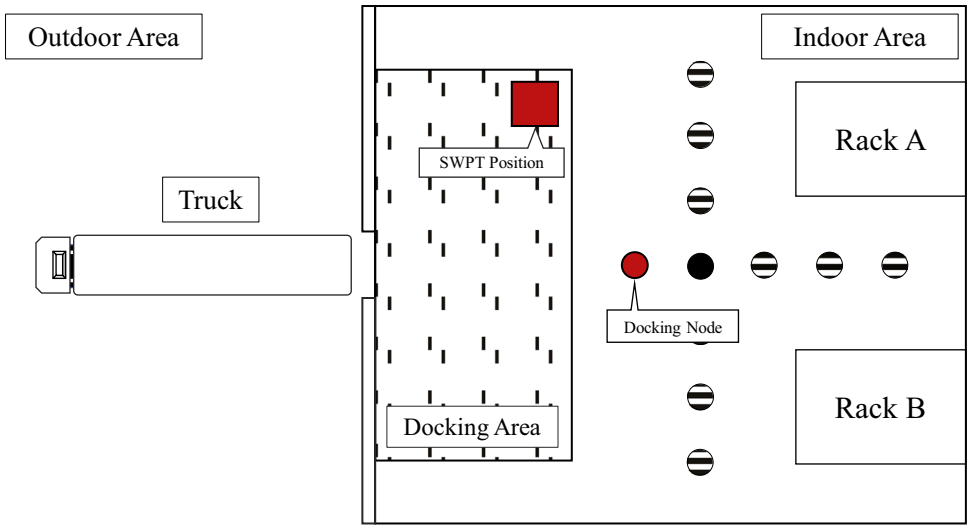

Fig. 4 Warehouse dock schematization (top view). The red square represents the possible position for the static coil, while the red dot represents the docking node, the node nearest to the docking area

- d_j: a sequential integer number starting from 1 representing the dock identifier.
- $dn_j \in N$: it identifies the docking node, i.e., the closest node to the working area.
- $dnf_j \in \{0, 1\}$: a docking node flag. This property is 1 if an SWPT charging point can be potentially installed on the dedicated area within the dock area, otherwise is 0.

As aforementioned, a docking node is a node nearer to the docking area. Any events that happen in the docking area are allocated to the corresponding docking node. It is assumed that SWPT chargers are mounted in dedicated areas where the forklift can remain stationary without impeding the execution of other operations. Figure 4 shows an example of dock configuration. The red dot represents the docking node, the big gray area represents the docking area, whereas the red square represents the transmitting part of an SWPT charger mounted on the dock area.

3.1.2 DWPT modeling

As a transmitting DWPT module is 2.5 m long, and the node spacing in the warehouse is 0.5 m, each transmitting DWPT module is composed of five consecutive nodes. It is convenient distinguishing the five nodes forming a DWPT module to correctly define a set of constraints that make the module physically installable. To this purpose, DWPT center is defined as the central node of the five consecutive nodes, whereas each of the other four nodes is identified as DWPT part. Moreover, a DWPT module can be oriented along the x-axis or y-axis.

According to the node category defined earlier, when all the nodes belonging to a DWPT module/section/transmitting section are horizontal or cross nodes, the module is called horizontal DWPT. When all the nodes belonging to a DWPT module are vertical or cross nodes, the module is called vertical DWPT. It turns out that a DWPT module can be uniquely identified by the position and orientation of its DWPT center.

Figure 5 shows an example of a possible DWPT module configuration. Red nodes are DWPT centers, whereas the blue ones are DWPT parts. Based on the above definition, it is possible to identify the DWPT sections displayed in Fig. 5 as a vertical DWPT with ID center 22, and a horizontal DWPT with ID center 12.

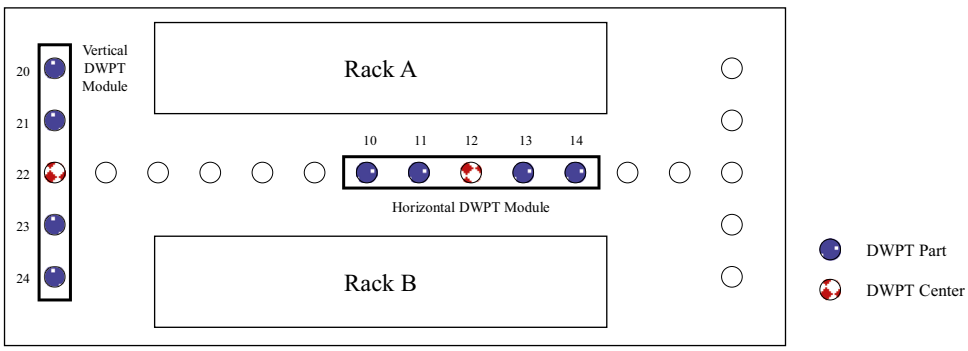

Fig. 5 DWPT configuration with vertical and horizontal DWPT modules, in blue DWPT part node, in red DWPT center node

3.1.3 Warehouse operation modeling

The two types of operations considered in this work are storing and retrieval operations. An operation starts and ends in the same docking node. Retrieval operations begin with the movement of the unloaded forklift from the loading dock to the retrieval point, i.e., the operational warehousing node (a warehousing node with *onf* equal to 1). Once arrived on it, the retrieval operation is executed, and the forklift is loaded with the item to be shipped. Finally, the forklift goes back to the loading dock and deposit the item on the truck. Conversely, storage operations begin with the movement of the loaded forklift from the docking node to the operational warehousing node. The item is stored in the warehouse, and then the unloaded forklift returns to the loading dock. The time spent by the forklift to cross a node in loaded and unloaded mode is assumed to be independent of the operation and depending only on the speed of the forklift; these quantities are, respectively, identified as loaded travel warehousing node time *ltwnt* and unloaded travel warehousing node time *utwnt*.

The path followed by the forklift during the execution of an operation can be the shortest between the two nodes, or it might be another one according to the warehouse policy. Anyway, neglecting the time difference between loading and unloading the item from the truck, as well as from the storage/retrieval point, from a temporal standpoint, the two types of operations can be treated as equivalents. So, it is possible to define a set of all the operations $\mathcal{O}$ with cardinality $|\mathcal{O}| = O$:

$$\mathcal{O} = \{1, 2, \dots, O\} \tag{6}$$

Each operation $k \in \mathcal{O}$ is characterized by the following properties:

- o_k: a sequential integer number starting from 1 representing the operation identifier.
- $odn_k \in \Delta$: the operational docking node, i.e., the dock where the item is loaded or unloaded during the operation.
- $own_k \in \mathcal{N}$: the operational warehousing node, i.e., the node where the item is stored or retrieved during the operation.
- $LWNP_k \subseteq \mathcal{N}$: the loaded warehousing nodes path, i.e., the set of nodes crossed during the path of the forklift in loaded conditions.
- $UWNP_k \subseteq \mathcal{N}$: the unloaded warehousing nodes path, i.e., the set of nodes crossed during the path of the forklift in unloaded conditions.
- $ownt_k$: the operational warehousing node time (in s), i.e., the time spent by the forklift in the operational warehousing node to store or retrieve the items.
- $odnt_k$: the operational docking node time (in s), i.e., the active time spent by the forklift in the dock to load or unload the item from the truck.
- ot_k: operation time, i.e., the total time of the operation (in s), that is the time spent by the forklift to move from the dock to the operational warehousing node and return to the dock, computed as follows:

$$\begin{aligned} ot_k = {} & ownt_k + odnt_k + ltwnt \cdot \left|LWNP_k\right| \\ & + utwnt \cdot \left|UWNP_k\right| \end{aligned} \tag{7}$$

- $op_k \in \{0, 1\}$: operation probability, which depends on the arrivals and retrievals of items in the warehouse.

Once nodes, edges, and operations have been characterized, the next methodological step is the probabilistic assessment of the electric forklift positions in a working shift within the modeled warehouse.

3.2 Probabilistic assessment of the forklift positions

The WPT modules are placed along with the most used nodes by the forklifts within the warehouse. In order to do that, the forklift's probability of being at a specific node must be assessed. This can be done by computing the time spent by the forklifts in each node during the execution of the operations. Such data can be collected in different ways, e.g., analytically through the study of the forklift paths if only the orders of the items to store/retrieve are known, numerically by means of a simulation model, or by embedding the forklifts with sensors to directly obtain the time spent in each position. Nevertheless, the methodology is suitable regardless of the system used for data collection activity.

3.2.1 Warehousing node probabilities

Assuming there is a set of forklifts $\mathrm{Z} = \{1, \dots, F\}$ in the warehouse, for each of them $f \in \mathrm{Z}$, it is possible to define a vector of N elements called warehousing node probabilities (WNP_f), a vector containing the probabilities to find a forklift located on warehousing nodes.

$$WNP_f = \left[\left(wnp_1\right)_f, \dots, \left(wnp_i\right)_f, \dots, \left(wnp_N\right)_f\right]^T \tag{8}$$

The probability of having a forklift in a warehousing node can be further divided into three parts. The operational warehousing node probabilities $OWNP_f$, i.e., the probability of having the forklift performing a storing or retrieval operation in the warehousing node, the loaded travel warehousing node probabilities $LTWNP_f$, i.e., the probability of having the forklift moving in loaded conditions across the space

covered by the warehousing node without stopping, and, finally, the unloaded travel warehousing node probabilities $UTWNP_f$, i.e., the probability of having the forklift moving in unloaded conditions across the space covered by the warehousing node without stopping. Thus, WNP_f can be written as the sum of such three terms:

$$WNP_f = OWNP_f + LTWNP_f + UTWNP_f \tag{9}$$

Each element of such vectors can be computed starting from the operation probability (op_k), the operation time $\left(ot_k\right)_f$, the operational warehousing node time $\left(ownt_k\right)_f$, the loaded travel warehousing node time $\left(ltwnt_k\right)_f$, and the unloaded travel warehousing node time $\left(utwnt_k\right)_f$, as reported below.

$$\left(ownp_i\right)_f = \begin{cases} \sum_{k=1}^{O} \frac{\left(ownt_k\right)_f}{\left(ot_k\right)_f} op_k, \ if\ i = own_k \\ 0, \qquad otherwise \end{cases} \quad \forall\, i \in \mathcal{N}, f \in \mathrm{Z} \tag{10}$$

$$\left(ltwnp_i\right)_f = \begin{cases} \sum_{k=1}^{O} \frac{\left(ltwnt\right)_f}{\left(ot_k\right)_f} op_k, \ if\ i \in LWNP_k \\ 0, \qquad otherwise \end{cases} \quad \forall\, i \in \mathcal{N}, f \in \mathrm{Z} \tag{11}$$

$$\left(utnp_i\right)_f = \begin{cases} \sum_{k=1}^{O} \frac{\left(utwnt\right)_f}{\left(ot_k\right)_f} op_k, \ if\ i \in UWNP_k \\ 0, \qquad otherwise \end{cases} \quad \forall\, i \in \mathcal{N}, f \in \mathrm{Z} \tag{12}$$

3.2.2 Docking node probabilities

A vector of D elements called operational docking node probabilities $(ODNP)_f$ can be defined for each forklift $f \in \mathrm{Z}$ as a vector containing the forklift's probability of being located on docking nodes during the operational phase.

$$ODNP_f = \left[\left(odnp_1\right)_f, \ldots, \left(odnp_j\right)_f, \ldots, \left(odnp_D\right)_f\right]^T \tag{13}$$

Each element of such vector can be computed starting from the operation probability op_k, the operation time $\left(ot_k\right)_f$, and the operational docking node time $\left(odnt_k\right)_f$. Mathematically,

$$\left(odnp_j\right)_f = \begin{cases} \sum_{k=1}^{O} \frac{\left(odnt_k\right)_f}{\left(ot_k\right)_f} op_k, \ if\ j = odn_k \\ 0, \qquad otherwise \end{cases} \quad \forall j \in \Delta, f \in \mathrm{Z} \tag{14}$$

Moreover, the probability of finding a forklift on a dock in waiting time can be collected in a vector called waiting docking node probabilities $WDNP_f$. Note that waiting time can be exploited by the forklift to statically recharge on a dock if there is an SWPT charging point on the dock.

3.2.3 Forklift's average behavior computation

After having carried out all the previous calculations, the mean behavior of the forklift must be assessed to build the future optimization problem. To this aim, the following average vector is computed.

$$WNP = \left[wnp_1, \ldots, wnp_i, \ldots, wnp_N\right]^T \tag{15}$$

WNP is the mean warehousing node probabilities vector, and its elements are evaluated as average over the values of forklifts.

$$wnp_i = \frac{1}{F} \sum_{f=1}^{F} \left(wnp_i\right)_f \forall i \in \mathcal{N} \tag{16}$$

In the same way, the vectors pertaining to loaded travel warehousing node probabilities *LTWNP*, unloaded travel warehousing node probabilities *UTWNP*, operational warehousing node probabilities *OWNP*, operational docking node probabilities *ODNP*, and waiting docking node probabilities *WDNP* are computed as average over the forklifts.

The six computed vectors characterize the mean behavior of the forklifts in the warehouse, and they will be used for the energetic balance described in the upcoming paragraph.

3.3 Energetic analysis

The most important constraint of the methodology is fulfilling the battery state of charge (SoC) variation of the forklifts in a working shift. So, the optimization algorithm would place the WPT module as the layout that satisfies the SoC variation required by the user, minimizing the cost based on the probabilistic assessment of the average forklift position discussed in the previous section.

Battery SoC, at any instant time, is defined as follows:

$$SoC = \frac{E_{batt}}{E_{batt,max}} \tag{17}$$

E_{batt} is the amount of energy stored in the battery at the considered instant time, whereas $E_{\mathrm{batt,max}}$ is the maximum capacity of the battery. It is possible to compute the SoC variation in a working shift $\Delta SoC_{\mathrm{shift}}$ as the difference between the absorbed energy $E_{\mathrm{IN,shift}}$ and the consumed energy $E_{\mathrm{OUT,shift}}$ in a working shift divided by the maximum capacity of the battery.

$$\Delta SoC_{\text{shift}} = \frac{\Delta E_{\text{shift}}}{E_{\text{batt,max}}} = \frac{E_{\text{IN,shift}} - E_{\text{OUT,shift}}}{E_{\text{batt,max}}} \tag{18}$$

The optimization algorithm will have to fulfill the following condition:

$$\Delta SoC_{\text{shift}} \geq \Delta SoC_{\text{shift,desired}} \tag{19}$$

3.3.1 Absorbed energy

During a working shift, the forklifts can be recharged in three different ways: (i) inside the warehouse on DWPT modules, (ii) during the waiting time on docks if the docks have an SWPT charging point, and, finally, (iii) during the break time if the forklifts are placed on SWPT charger in docks.

The absorbed energy taken directly from the DWPT module can be computed as follows:

$$E_{\text{IN,dyn}} = \eta_{\text{dyn}} \cdot P_{\text{nom}} \cdot ST_{\text{eff}} \cdot \sum_{i=1}^{N} \left(wnp_i \cdot x_i \right) \tag{20}$$

where η_{dyn} is the efficiency of the DWPT system, P_{nom} is the nominal DWPT system charging power, ST_{eff} is the effective working shift duration, and x_i is a binary variable equal to 1 when a DWPT module is placed on the i-th node, 0 otherwise. x_i represents a variable to be optimized during the optimization process.

The absorbed energy during the waiting time in docks $E_{\text{IN,static,waiting}}$ in a working shift is computed similarly.

$$E_{\text{IN,static,waiting}} = \eta_{\text{static}} \cdot P_{\text{nom}} \cdot ST_{\text{eff}} \cdot \sum_{j=1}^{D} \left(wdnp_j \cdot xd_j \right) \tag{21}$$

where η_{static} is the efficiency of the SWPT system, ST_{eff} is the effective working shift time, whereas xd_j is a flag equal to 1 when an SWPT system is placed on j-th dock, 0 otherwise. Note that xd_j is an optimization variable, too.

The absorbed energy during the breaks $E_{\text{IN,static,breaks}}$ can be computed as follows:

$$E_{\text{IN,static,breaks}} = k_{\text{breaks}} \cdot \eta_{\text{static}} \cdot P_{\text{nom}} \cdot BT \tag{22}$$

where k_{breaks} accounts for the effective proportion of forklifts that can be recharged during the breaks, and BT is the break time duration in a working shift.

Finally, the three contributions are summed up:

$$E_{\text{IN,shift}} = E_{\text{IN,dyn}} + E_{\text{IN,static,waiting}} + E_{\text{IN,static,breaks}} \tag{23}$$

3.3.2 Consumed energy

In a working shift, four sources of energy consumption are modeled in this work: (i) the execution of an operation in the dock, (ii) the execution of an operation in the warehousing node, (iii) the forklift motion within the warehouse in loaded conditions, and (iv) the forklift motion within the warehouse in unloaded conditions.

The energy lost during the loading/unloading phase in docks ($E_{\text{OUT,odn}}$) can be computed in the following way.

$$E_{\text{OUT,odn}} = P_{\text{cons,odn}} \cdot ST_{\text{eff}} \cdot \sum_{j=1}^{D} odnp_j \tag{24}$$

$P_{\text{cons,odn}}$ is the electrical power required for the execution of an operation in dock.

In an analogous way can be assessed the energy spent during the forklift motion in loaded conditions $E_{\text{OUT,ltwn}}$ and unloaded conditions $E_{\text{OUT,utwn}}$, as well as the energy spent by the forklift during the execution of an operation in warehousing nodes $E_{\text{OUT,own}}$.

$$E_{\text{OUT,own}} = P_{\text{cons,own}} \cdot ST_{\text{eff}} \cdot \sum_{i=1}^{N} ownp_i \tag{25}$$

$$E_{\text{OUT,ltwn}} = P_{\text{cons,ltwn}} \cdot ST_{\text{eff}} \cdot \sum_{i=1}^{N} ltwnp_i \tag{26}$$

$$E_{\text{OUT,utwn}} = P_{\text{cons,utwn}} \cdot ST_{\text{eff}} \cdot \sum_{i=1}^{N} utwnp_i \tag{27}$$

$P_{\text{cons,own}}$, $P_{\text{cons,ltwn}}$, and $P_{\text{cons,utwn}}$ are, respectively, the electric power needed to carry out an operation in warehousing nodes, the electric power needed by the forklift to travel within the warehousing nodes in loaded conditions, and the electric power needed by the unloaded forklift to travel within the warehousing nodes.

As for the acquired energy, all the contributions are summed up.

$$E_{\text{OUT,shift}} = E_{\text{OUT,odn}} + E_{\text{OUT,own}} + E_{\text{OUT,ltwn}} + E_{\text{OUT,utwn}} \tag{28}$$

3.4 Optimization problem

The objective of the optimization problem is to define a mathematical model to be optimized based on the definitions discussed in the previous section. The final goal is to find a physically installable placement of the WPT system layout to fulfill the energetic constraint required by the customer to minimize the cost of the system. The problem is modeled as an integer linear programming (ILP) problem in which a linear function must be minimized by fulfilling a set of constraints made of linear equalities and inequalities.

Because the working area is discretized in N warehousing nodes and D docking nodes, the following set of optimization variables θ can be defined.

$$\theta \in \mathbb{R}^{5N+D} \; : \; \theta = \{\theta_1, \ldots, \theta_{5N+D}\} \tag{29}$$

Each optimization variable is a binary variable that can be equal to 0 or 1, and because of this, the problem is defined as integer linear programming (ILP). The set θ of optimization variables can be split into six subsets and arranged in the following column vector.

$$\begin{aligned}\theta = [&x_1, \ldots, x_N, h_1, \ldots, h_{N,}, hc_1, \ldots, hc_N, v_1, \ldots, \\ &v_N, vc_1, \ldots, vc_N, xd_1, \ldots, xd_D]^T\end{aligned} \tag{30}$$

Each subset variable has the following meaning:

- x_i is 1 if a DWPT module is placed on node i, otherwise is 0.
- h_i is 1 if a horizontal DWPT part is placed on node i, otherwise is 0.
- hc_i is 1 if a horizontal DWPT center is placed on node i, otherwise is 0.
- v_i is 1 if a vertical DWPT part is placed on node i, otherwise is 0.
- vc_i is 1 if a vertical DWPT center is placed on node i, otherwise is 0.
- xd_j is 1 if an SWPT module is placed on dock j, otherwise is 0.

Note that if one of the optimization variables h_i, hc_i, v_i, vc_i is 1, so x_i must be 1, too.

The cost function of the optimization problem is a linear function representing the overall cost of the WPT system; it is defined as follows.

$$f(\theta) = c^T\theta \tag{31}$$

c is the cost vector representing the cost of each optimization variable. It can be arranged as follows.

$$c = [c_1, \ldots, c_i, \ldots, c_{5N+D}]^T \tag{32}$$

$$\text{with} \quad c_i = c_{\text{dyn}} \quad i \in \mathcal{N} : 1 \le i \le N \tag{32a}$$

$$c_i = 0 \;\; i \in \mathcal{N} : N+1 \le i \le 5N \tag{32b}$$

$$c_i = c_{\text{static}} \;\; i \in \mathcal{N} : 5N+1 \le i \le 5N+D \tag{32c}$$

c_{dyn} is the cost of a DWPT module and, c_{static} is the cost of an SWPT module.

The final formulation of the cost function, considering only the non-null costs, is reported below.

$$f(\theta) = \sum_{i=1}^{N} \left(c_{\text{dyn}} \cdot x_i\right) + \sum_{j=1}^{D} \left(c_{\text{static}} \cdot xd_j\right) \tag{33}$$

The model is subjected to a set of constraints, many of which are topological.

If a node is a horizontal node, then it can just be a horizontal part or horizontal center of a DWPT module (38a). The same happens for what concerns the vertical direction modeled (38b), whereas if a node is a cross node, both directions are allowed, and that node could be a horizontal part, or horizontal center, or vertical part, or vertical center (38c).

If a node belongs to the 4th category, no DWPT module can be installed on that node (38d).

Relating to corridors, in any horizontal corridor, the sum of all the horizontal DWPT parts must be 4 times the sum of all the horizontal DWPT centers (38e). The same condition must be applied for vertical corridors, too (38f).

Additionally, some constraints must be described to force the creation of the DWPT module as a strip of five consecutive nodes. To this aim, we define the distance matrix of the node of the graph as $C = (c_{i_1 i_2})$, C is a positive and symmetric $N \times N$ matrix. Each value represents the minimum distance in steps between the two nodes i_1 and i_2, and all the entities on the main diagonal are equal to 0. For each $\bar{\imath} \in \mathcal{N}$ it is possible to define four different sets of nodes: *radius-2 horizontal neighbors* of node $\bar{\imath}$ ($R^{2h}_{\bar{\imath}}$), *radius-2 vertical neighbors* of node $\bar{\imath}$ ($R^{2v}_{\bar{\imath}}$), *distance-5 horizontal neighbors* of node $\bar{\imath}$ ($L^{5h}_{\bar{\imath}}$), and *distance-5 vertical neighborhood* of node $\bar{\imath}$ ($L^{5v}_{\bar{\imath}}$)

$$R^{2h}_{\bar{\imath}} = \left\{\forall i \in \mathcal{N} : i \ne \bar{\imath}, horoc_i \ne 0, horoc_{\bar{\imath}} = horoc_i, c_{\bar{\imath}i} \le 2\right\} \tag{34}$$

$$R^{2h}_{\bar{\imath}} = \left\{\forall\, i \;\in\; \mathcal{N} : i \ne \bar{\imath}, verc_i \ne 0, verc_{\bar{\imath}} = verc_i, c_{\bar{\imath}i} \le 2\right\} \tag{35}$$

$$L^{5h}_{\bar{\imath}} = \{\forall i \in \mathcal{N} : i \ne \bar{\imath}, horoc_i \ne 0, horoc_{\bar{\imath}} = horoc_i, c_{\bar{\imath}i} = 5\} \tag{36}$$

$$L^{5v}_{\bar{\imath}} = \{\forall i \in \mathcal{N} : i \ne \bar{\imath}, verc_i \ne 0, verc_{\bar{\imath}} = verc_i, c_{\bar{\imath}i} = 5\} \tag{37}$$

Following such definitions, when a node is a *horizontal DWPT center*, it must have four *radius-2 horizontal neighbors*, and all of them must be *horizontal DWPT parts*, as well as when a node is a *vertical DWPT center*, it must have four *radius-2 vertical neighbors*, all of them must be *vertical DWPT parts*. These constraints are, respectively, represented in Eqs. (38g) and (38h). Equations (38i) and (38j) force each DWPT part to have precisely one DWPT center among the nodes belonging to its *radius-2 neighborhood*. The DWPT module length for horizontal DWPTs is constrained in Eqs. (38k) and (38l), whereas the DWPT module length for vertical DWPTs is constrained in Eqs. (38m) and (38n). In some docks, it is not possible to install any SWPT module. This is defined

in (38o). The energetic constraint required by the customer is modeled in (38p). Finally, the constraint pertaining to the binary integer values of the optimization variables is defined in the last constraint (38q).

$$3x_i - 3h_i - 3hc_i - v_i - vc_i = 0 \ \forall i \in \mathcal{N} : cat_i = 1 \tag{38a}$$

$$3x_i - h_i - hc_i - 3v_i - 3vc_i = 0 \ \forall i \in \mathcal{N} : cat_i = 2 \tag{38b}$$

$$x_i - h_i - hc_i - v_i - vc_i = 0 \ \forall i \in \mathcal{N} : cat_i = 3 \tag{38c}$$

$$x_i + h_i + hc_i + v_i + vc_i = 0 \ \forall i \in \mathcal{N} : cat_i = 4 \tag{38d}$$

$$\sum_{i=1}^{N} (h_i) - 4 \sum_{i=1}^{N} (hc_i) = 0 \ \forall i \in \mathcal{N} : horc_i = h, h \epsilon \mathcal{H} \tag{38e}$$

$$\sum_{i=1}^{N} (v_i) - 4 \sum_{i=1}^{N} (vc_i) = 0 \ \forall i \in \mathcal{N} : verc_i = v, v \epsilon \mathcal{V} \tag{38f}$$

$$4hc_i - \sum_z h_z \leq 0 \ \forall i \in \mathcal{N}, \forall z \in R_i^{2h} : \left| R_i^{2h} \right| = 4 \tag{38g}$$

$$4vc_i - \sum_z v_z \leq 0 \ \forall i \in \mathcal{N}, \forall z \in R_i^{2v} : \left| R_i^{2v} \right| = 4 \tag{38h}$$

$$h_i - \sum_z hc_z \leq 0 \ \forall i \in \mathcal{N}, \forall z \in R_i^{2h} : cat_i \in \{1, 3\} \tag{38i}$$

$$v_i - \sum_z vc_z \leq 0 \ \forall i \in \mathcal{N}, \forall z \in R_i^{2v} : cat_i \in \{2, 3\} \tag{38j}$$

$$hc_i - \sum_z hc_z \leq 0 \ \forall i \in \mathcal{N}, \forall j \in L_i^{5h} : cat_i \in \{1, 3\}, L_i^{5h} \neq \varnothing \tag{38k}$$

$$hc_i = 0 \ \forall i \in \mathcal{N} : cat_i \in \{1, 3\}, L_i^{5h} = \varnothing \tag{38l}$$

$$vc_i - \sum_z vc_z \leq 0 \ \forall i \in \mathcal{N}, \forall j \in L_i^{5v} : cat_i \in \{2, 3\}, L_i^{5v} \neq \varnothing \tag{38m}$$

$$vc_i = 0 \ \forall i \in \mathcal{N} : cat_i \in \{2, 3\}, L_i^{5v} = \varnothing \tag{38n}$$

$$xd_j = 0 \ \forall j \in \Delta : dwf_j = 0 \tag{38o}$$

$$E_{\text{IN,shift}} \geq E_{\text{OUT,shift}} \tag{38p}$$

$$x_i, h_i, hc_i, v_i, vc_i, xd_j \in \{0, 1\} \forall i, \forall j \tag{38q}$$

The optimal solution corresponds to the overall cost of the whole WPT system.

$$f_{\text{MIN}} = \min \left(\sum_i c_d x_i + \sum_j c_s x d_j \right) = cost_{\text{tot}} \tag{39}$$

$$\sum_i c_d x_i = cost_{\text{dyn}} \tag{39a}$$

$$\sum_j c_s x d_j = cost_{\text{stat}} \tag{39b}$$

Such an optimization model has been implemented in Matlab (https://mathworks.com/)

4 Case study

The proposed approach was applied in an industrial case study to optimize the installation of a WPT system (SWPT + DWPT systems) in the full-scale dimension warehouse used as a distribution center by a tire manufacturer company. The case study is appropriately modified to protect the company's privacy; nevertheless, the study does not lose its significance.

4.1 Warehouse description

The warehouse object of this work is displayed in Fig. 6. It has a rectangular shape: the long side measures 245 m, and the short one is 183 m. It presents 16 docks (they are evidenced with a capital D in the figure), 8 on each of the long sides. The docks are directly connected to the outside, and each one can accommodate a truck waiting to be loaded. There are two different forklift parking spaces on the

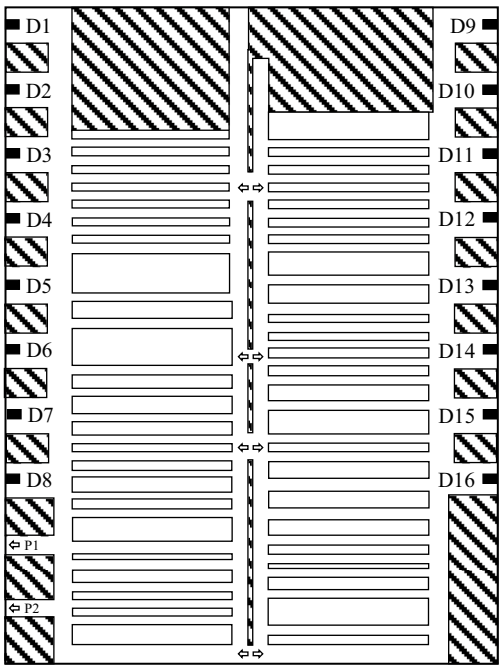

Fig. 6 Warehouse layout

warehouse's left side (marked with a capital P). The building is divided into two zones separated by a central wall. It is possible to change the zone using one of the four gates. These wall passages are placed at the bottom, one at the top, and two in the middle of the warehouse (in the figure, they are highlighted with two opposing arrows). The warehouse has 94 racks 60 m long, 8.4 m tall, and depth between 1.5 m and 9 m. In the figure, racks are represented by white boxes. Each rack has 6 levels and 24 bays. The unit load (UL) is composed of eight pairs of tires, fastened by belts and placed on a pallet. The maximum volume of each UL is 1.728 m^3, a cube with each edge 1.2 m long. The warehouse can store 41.184 ULs.

4.2 Experimental tests of forklift consumption

The electric forklift taken as reference is the Toyota Traigo 48 [34], and all parameters are based on this model. These forklifts have a load capacity of 1600 kg, their weight (battery included) is equal to 3002 kg. According to the technical specifications, Toyota Traigo mounts two traction motors with nominal power equal to 6 kW each and a lifting motor with nominal power equal to 11 kW. Each vehicle mounts a 48 V battery with a capacity of 30 kWh.

According to the VDI (Verband Deutscher Ingenieure) cycle [35], the average power is 4.3 kWh/h. However, this cycle is particularly energy intensive; it involves a series of movements and lifts to obtain a power parameter that can indicate an average energy consumption. This average consumption is obtained simulating a too stressful use that in practice is never found. For this reason, a battery charge cycle analysis is performed; real charge and discharge data of the batteries have been collected on two forklifts in a real operating environment through the control unit of the forklift instrumentation. The studied forklifts were equipped with a 48-V hermetic lead-acid battery consisting of 24 cells, with a capacity of 30 kWh. The obtained results have been averaged and reported in Table 1.

These vehicles have a maximum speed of 16 km/h. However, 5 km/h is the most common speed limit in an indoor warehouse where pedestrians are present. The vehicle's lift speed is 0.50 m/s.

Table 1 Experimental results of forklift consumption

	Value
Average consumed energy per cycle	26.17 kWh
Maximum consumed energy	52.15 kWh
Minimum consumed energy	3.23 kWh
Average experimental total power	2.82 kWh/h
Average experimental traction power	2.48 kWh/h
VDI cycle power	4.30 kWh/h

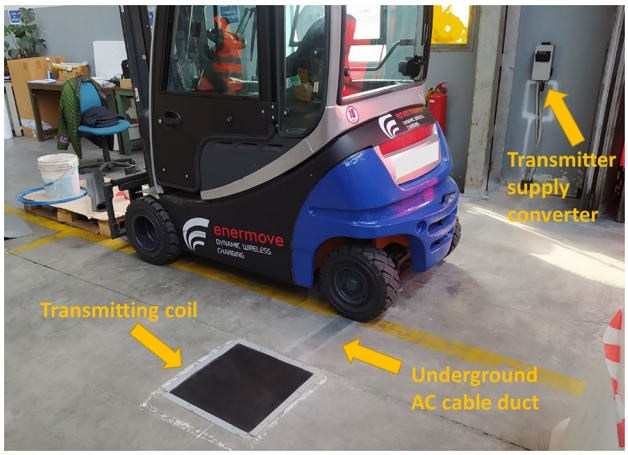

Fig. 7 Forklift in an industrial environment with a detail of an SWPT charging point

4.3 WPT parameters

In this section, all the WPT system parameters used in the case study are described (Table 2). Such data is provided by the Italian company Enermove srl. Figure 7 shows the forklift analyzed in this study equipped with a WPT system developed by Enermove. The SWPT module is shown in the figure, and it results in a square base having a size 45 cm × 45 cm at the same level of the floor.

The transmitting pad of the DWPT system has a length of 120 cm and a width of 20 cm. The forklift operates with both static and dynamic WPT systems through the same receiver, having a square shape with each side 35 cm wide, and it is mounted underneath the vehicle chassis. In the analyzed case study, each WTP module (both dynamic and static) has a rated charging power equal to 3.5 kW. The efficiency of the DWPT transmission is around 85%, while SWPT is about 90%. The deployment of dynamic transmitting coils requires a minor cut on the concrete superficial layer to create a slot to place the coil. Then, the coil is molded in a specific resin and subsequently covered by concrete or a layer of resin for

Table 2 WPT systems' parameters

Parameter	Value
DWPT module dimension	2.50 m × 0.20 m
DWPT module power (P_{nom})	3.5 kW
DWPT efficiency (η_{dyn})	0.85
DWPT module cost (c_{dyn})	2500 €
SWPT module dimension	0.45 m × 0.45 m
SWPT module power (P_{nom})	3.5 kW
SWPT efficiency (η_{stat})	0.90
SWPT module cost (c_{static})	3000 €

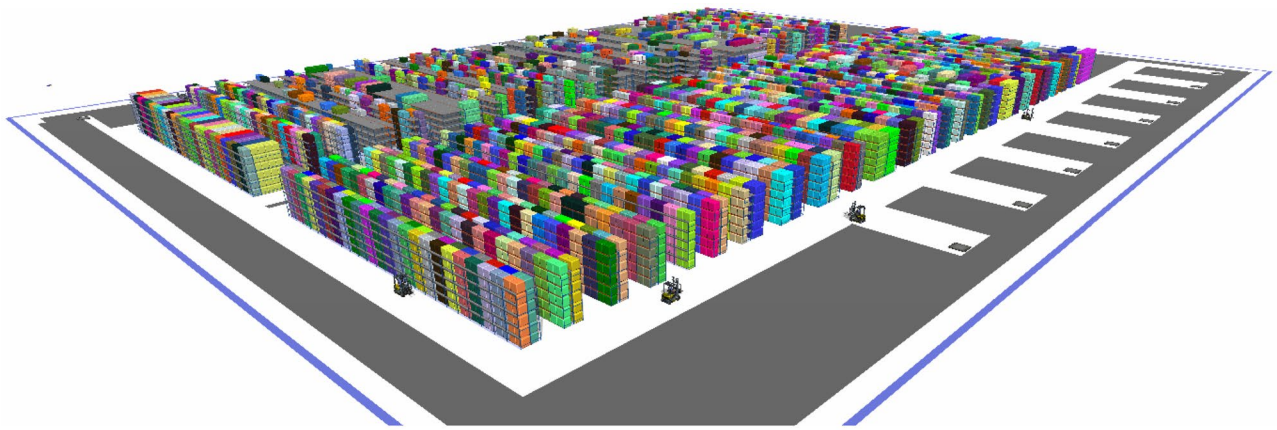

Fig. 8 Warehouse simulation model

industrial pavements. Hence, no further maintenance operations are required on the coils as they remain embedded in the pavement during the whole service life of the WPT system. On the other side, a static transmitter may also be mounted without creating any slot in the concrete in the so-called above-ground installation mode in which the receiver coil assembly is directly bolted to the pavement.

As the DC/AC converter can simultaneously manage two transmitting coils, mounted sequentially and adjacent to each other, a length of 2.5 m has been chosen for the DWPT module. A medium gap of 0.1 m has been considered to allow the correct assembly of the components on the floor. Note that the dimension of the transmitters listed at the beginning of this section, the DWPT module length, can vary slightly according to the specific application. The cost of each DWPT transmitting module is 2500 €. An SWPT transmitter costs 3000 €, while the cost of the receiver to be mounted on the forklift is 1500 €.

4.4 Model application

In order to evaluate the model in different warehouse conditions, a discrete event simulation model of the full-scale dimension warehouse was developed by using the Flexsim software (https://www.flexsim.com). The whole warehouse is modeled using 11094 nodes (11078 warehousing nodes and 16 docking nodes) and 11264 edges. In Fig. 8, we present the build warehouse model during a simulation run.

In order to simulate the warehouse, we have had to specify some logic and behaviors. Moreover, we have based on some previously described assumptions. In this paragraph, we report all the parameters and the logic used to model the warehouse.

Each replication represents a stand-alone shift from 8 A.M to 4 P.M., at the beginning of the shift, the total units stored are 30.888 (75% of the full capacity). We decided to simulate only retrieval tasks performed by 4 forklifts. Orders arrive following an exponential distribution with an expected value of $1/\lambda$. When an order comes, if there is space, a dock is reserved. Otherwise, the order waits until one of the sixteen docks is back available. When an order enters the port, the forklift is called back to the dock to receive the details. Forklifts retrieve the items in the warehouse according to a minimum travel distance law. Each order is composed of a single homogeneous unit load. Tasks are managed according to a FIFO rule.

Loading and unloading procedure time follows a log-normal distribution with an expected value equal to 20 s and a variance equal to 16 s^2. The vehicles move in straight lines and 90° curves; diagonal movements are not allowed. This behavior is in line with the traffic rules of the existing warehouses and the general safety requirements. A forklift moves from point A to point B via the shortest path in each task. The shortest path is computed using the A* algorithm [36]. We have modeled a forklift driver break behavior. On average, the drivers take a break every 90 min. When a task is finished, the driver stops the forklift near the dock if 90 min are passed from the previous break. The pause time follows an exponential distribution with an expected value equal to 15 min. We let the possibility of skipping breaks. If the driver is performing a particularly long task and the break time has already passed by several minutes at the end of this task, the driver will continue working. This behavior makes the model more realistic and less mechanistic.

Table 3 Warehouse parameters

Parameter	Value
Warehouse dimensions	240–183 m
Total unit load capacity	41184
Space utilization	75%
Standard unit load volume	1.728 m^3

Table 4 Forklift parameters

Parameter	Value
Max speed	5 km/h
Lift max speed	0.5 m/s
$P_{cons,ltwn}$	4.30 kWh/h
$P_{cons,utwn}$	1.23 kWh/h
$P_{cons,own}$	3.92 kWh/h
$P_{cons,odn}$	3.92 kWh/h
Battery capacity	30 kWh

From the energy point of view, we based the energy consumption on the average experimental total power (2.82 kWh/h) and the average experimental traction power (2.48 kWh/h) and the VDI cycle power (4.30 kWh/h) described previously. In order to be as conservative as possible, we decided to use a power equal to 4.30 kWh/h as the average power travel loaded ($P_{cons,ltwn}$). In order to figure the energy consumption of each shift, we need to find the three missing powers: (i) average power travel unloaded ($P_{cons,utwn}$), (ii) average power for warehouse operations ($P_{cons,own}$), and (iii) average for dock operations ($P_{cons,odn}$). It has been assumed that an equal power value for $P_{cons,own}$ and $P_{cons,odn}$ since the forklift operations are the same; it only changes the area they are completed. Then, $P_{cons,utwn}$ and $P_{cons,own}$ have been computed by solving the following equations:

$$\begin{cases} \frac{UTWNP}{LTWNP+UTWNP}P_{cons,utwn} + \frac{LTWNP}{LTWNP+UTWNP}P_{cons,ltwn} = 2.48kWh/h \\ \frac{UTWNP}{WNP+ODNP}P_{cons,utwn} + \frac{LTWNP}{WNP+ODNP}P_{cons,ltwn} + \frac{OWNP}{WNP+ODNP}P_{cons,own} + \frac{ODNP}{WNP+ODNP}P_{cons,odn} = 2.82kWh/h \end{cases} \quad (40)$$

The main warehouse parameters used in the simulation model are described in Table 3, while Table 4 shows the forklift parameters.

In order to assess the methodology and its robustness in different operating conditions of the warehouse, we define two distinct scenarios (A and B), depending on the order interarrival rate of orders and the storage logic of SKUs in the warehouse. Scenario A has a high interarrival rate, while scenario B has a low interarrival rate. In scenario A, items are placed randomly with three degrees of freedom, while in scenario B, the degrees of freedom are only two: objects in the same bay must be homogeneous. A scheme of these two logics is represented in Fig. 9. Having three degrees of freedom allows the management of more SKU types than the logic with only two degrees of freedom since, in the same space, it is possible to store a more significant number of unique SKUs. So, another difference between scenarios A and B is the number of unique SKUs stored.

An outline of the two scenarios is reported in Table 5.

The simulation output is a warehouse heatmap: we have simulated positioning sensors that update the forklift positions every 0.25 s. On each update, sensors record the forklift ID, its *x* and *y* positions in the warehouse, the state in which the forklift is (idle, travel empty, loading, travel loaded, unloading, and on break), and the total travel distance from the beginning of the simulation.

For each analyzed scenario, 60 simulations were run: 30 of them were used to assess the probabilities of the forklift positions to feed the optimizer, while the other 30 simulations were used to validate the optimizer results, keeping track of the state of charge of the forklifts' battery.

5 Results and discussion

This section presents the work results, i.e., the optimal WPT layout with the associated cost and the state of charge verification of the forklifts. In order to achieve the optimal solution, we use the Matlab function *intlinprog*. The results have been obtained with a computer HP 290

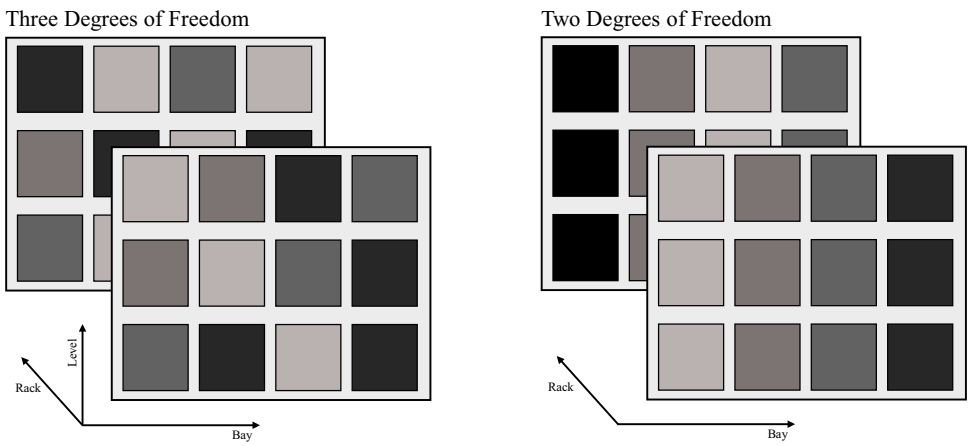

Fig. 9 The two warehouse storage logics

Table 5 Explored scenarios

Parameter	Scenario A	Scenario B
Interarrival ($1/\lambda$)	70 s	10 s
SKU number	500	100
Storage DoF	3	2

G4 Microtower, with CPU Intel core i7-10700 2.90 GHz and RAM 64 GB. The average time required by the computer to generate the entire graph and build the constraints was approximately 4 h and 15 min. The algorithm managed to find the optimal solutions in about 5 min and 26 s.

Section 5.1 reports the results obtained by the optimizer. As previously described, the optimizer needs as input five different elements. (i) The discretized warehouse, an un-oriented graph composed of N node, E arcs and D docking node. (ii) The four vectors defining the forklifts' status: $OWNP_f$ defining the probability of having the forklift operating a specific warehousing node, $LTWNP_f$ representing the probability of having a loaded forklift moving across the space covered by the warehousing node, $UTWNP_f$ i.e., the probability of having the forklift moving unloaded across the space covered by the warehousing, and finally, the vector $ODNP_f$ defining the probability of having the forklift operating in a particular dock. To estimate these four vectors, we use the first set of 30 simulations. (iii) The WPT system characterization: the DWPT and SWPT model dimension, power efficiency, and cost. (iv) The forklift consumption behavior, in particular, the average power needed to move the forklift loaded ($P_{\text{cons,ltwn}}$), unloaded ($P_{\text{cons,ltwn}}$), and to handle UL in the warehouse ($P_{\text{cons,own}}$) and the docking ($P_{\text{cons,odn}}$) and, finally, (v) the energetic constraint. In our case study, we have imposed a change in battery state of charge equal to 0 during a shift ($E_{\text{IN,shift}} \geq E_{\text{OUT,shift}}$). The output of the optimizer is the decision variables x_i and xd_j, indicating whether the DWPT or SWPT systems are present in the i -th node and j-th docking node.

Section 5.2 presents the validation of the obtained solution. We validate our solutions by analyzing the second set of 30 simulations, each lasting 8 h. We give as input for the simulator the obtained optimal distribution of DWPT and SWPT, and we compute the state of charge time series of the 4 forklifts present in each simulation. The model is validated whether, on average, the consumption of the forklifts is equal to the energy recharged. Furthermore, knowing the trend of all 120 SoC curves (30 simulations for 4 forklifts) allows us to evaluate the robustness of the obtained solution. If the SoC drop to zero, even a single time for a shift, this would mean a failure of the obtained solution. As previously mentioned, the analysis is performed on two separate scenarios.

5.1 WPT layout and cost

For the analyzed scenarios in this work, the optimizer has computed the whole WPT system layouts schematically represented in Fig. 10. It is possible to observe, for both scenarios, that it is placed the SWPT charger in each docking area. Moreover, the figure displays that DWPT modules are mainly located in the two lateral corridors and at the end part of the aisles between racks. This behavior is due to using the shortest path logic assumed by forklifts in

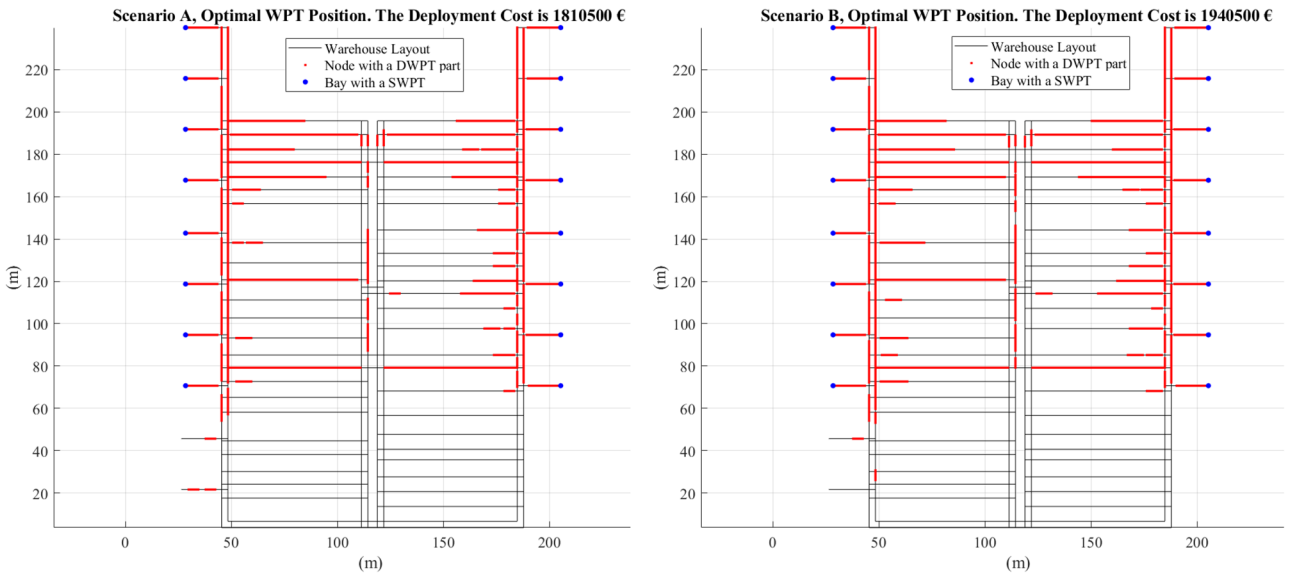

Fig. 10 Optimal WPT layout, scenario A ($1/\lambda = 70$ s) on the left and scenario B ($1/\lambda = 10$ s) on the right

Table 6 Optimal results

Parameter	Scenario A	Scenario B
Number of DWPT modules	705	757
Number of SWPT chargers	16	16
Length of DWPT system	1762.5 m	1892.5 m
Cost of DWPT system	1,762,500 €	1,892,500 €
Cost of SWPT system cost	48,000 €	48,000 €

the simulation; the vehicles transit mainly near the docking area and the adjacent area.

Notably, for what concerns scenario A, 705 DWPT modules have been placed inside the warehouse, corresponding to a total length of 1762.5 m and associated cost of 1,762,500 €, while 16 SWPT chargers are needed in docking areas with a cost of 48,000 €. Regarding scenario B, 757 DWPT modules have been calculated by the optimizer, corresponding to a total length of about 1892.5 m and an associated cost of 1,892,500 €, while 16 SWPT chargers in docking areas and a cost of 48,000 €. We analyzed two extreme scenarios where the order frequency between scenarios A and B increased seven times. Despite this radical difference, the final result in terms of cost differs by less than 10% (7.18%). This result shows the remarkable robustness of the obtained solution. If the warehouse has an extreme variable demand with interarrival of orders very different every day, there is a low risk of having an insufficient WPT number. Table 6 summarizes the achieved results.

Concerning the case study analyzed in this work, the methodology developed and the results obtained lead to consider the use of WPT charging systems as very promising. Compared to the current charging procedure used (battery swap and fast charging), the wireless method has numerous advantages over its operational life cycle, despite a higher initial investment cost. In particular, both battery swap and fast charging require the use of one or more operators who have to deal with a non-added value activity for a considerable time. In the case of battery swap, there is also a significant safety concern in battery connection, disconnection, and handling procedures. Furthermore, both traditional systems also require considerable investment. Fast charging needs installing a higher-powered electrical system and a series of fast charger points. Moreover, the utilization of forklifts will be lower, which means that a more significant number of forklifts will be needed. Finally, with regard to the battery swap, a considerable investment is the set of spare batteries to be purchased, stored, and managed. A complete economic comparison between the WPT charging system and traditional ones will be the object of future studies.

5.2 State of charge verification

Once the optimal distribution of SWPT and DWPT modules was obtained, we analyzed the outputs of 30 simulations for each simulated scenario for a total of 60 simulations. The aim is to monitor the evolution of the SoC variation for each forklift and check if the methodology proposed in this work

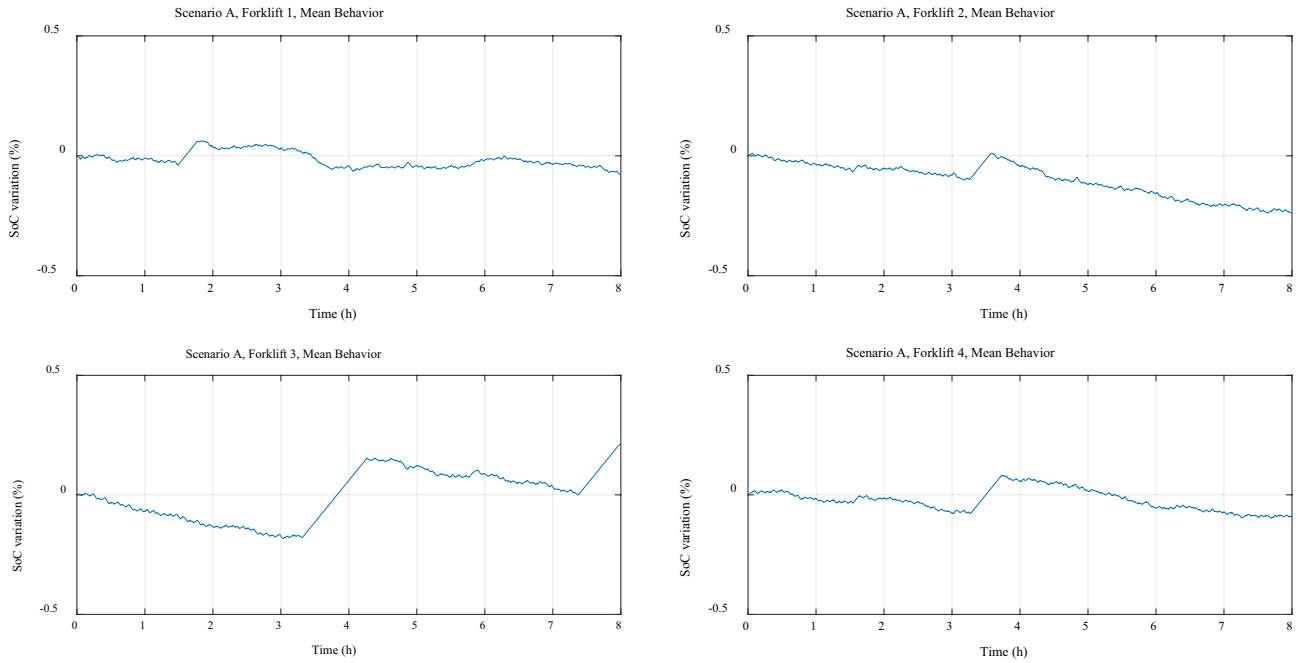

Fig. 11 SoC variation in the average working shift for scenario A

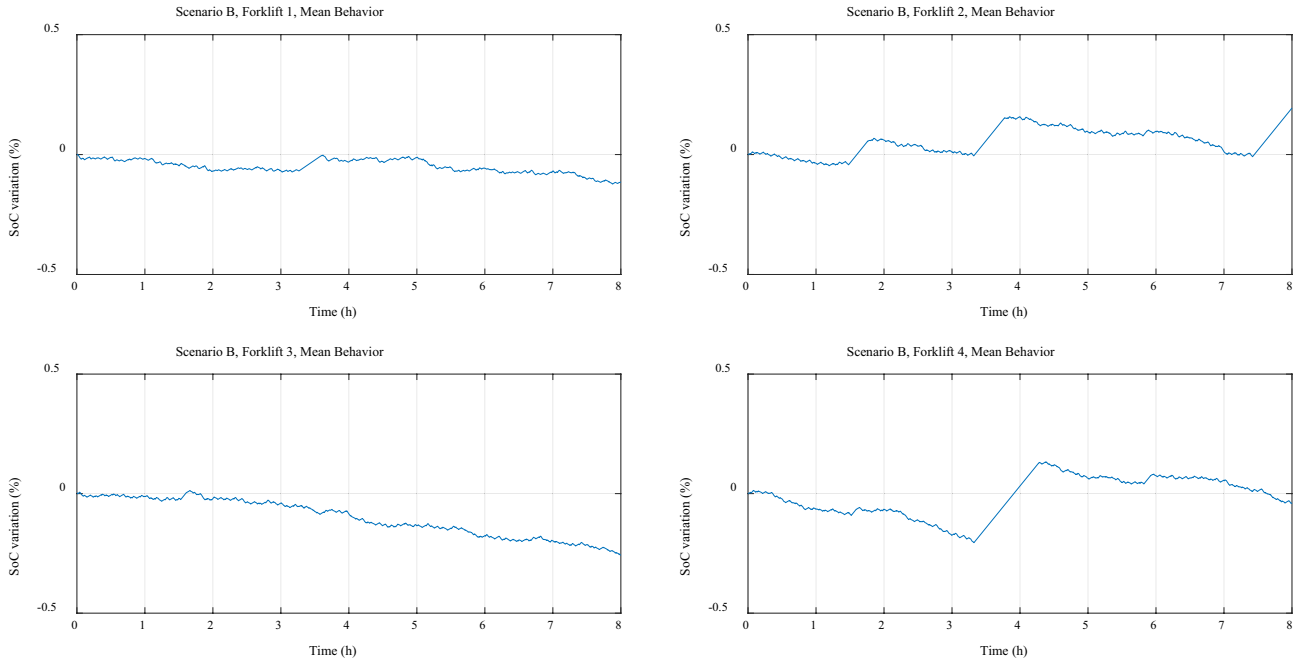

Fig. 12 SoC variation in the average working shift for scenario B

is effective. Each scenario has been averaged on its 30 working shifts to track the forklifts' mean behavior. The results are shown in Figs. 11 and 12, respectively, for scenarios A and B. On average, all forklifts have an SoC variation within ± 0.5%, which can be considered a satisfactory result. Moreover, almost all forklifts are generally characterized by charging spikes; this behavior is due to driver breaks.

Analyzing the 120 forklifts' SoC, we noticed that the battery never dropped to zero. Moreover, Table 7 summarizes the maximum and minimum SoC variation detected for each scenario. As it is possible to observe, the proposed methodology guarantees a constant availability of electric vehicles even in extreme cases. Indeed, in the worst case, the minimum SoC variation is – 15.86%, and, assuming an initial reference SoC of about 50%, it led to a residual SoC of the forklift above 30%. This behavior is highly reassuring; the most extreme cases are far above a level of risk, so the possibility of forklifts ending up mid-shift with a dead battery is very low, considering the positioning of the coils obtained from the optimizer.

Since the analyzed warehouse is very complex and has a considerable dimension, the obtained results reveal an excellent performance of the proposed methodology. In smaller warehouses, the difference between the behavior of the single forklift and the mean behavior of the forklifts is likely limited, and so the current methodology is expected to be reliable also in a warehouse with reduced size.

Table 7 Maximum and minimum SoC variation detected for each scenario

	Scenario A	Scenario B
Max	+ 18.63 %	+ 22.98 %
Min	– 11.95 %	– 15.86%

6 Conclusions and future improvements

This work proposes a design methodology for the computation of the optimal static and dynamic WPT system layout based on the usage map of the electric vehicles within the working area. The procedure has been virtually applied to a case study involving a real warehouse layout, real electric forklifts data, as well as real static and dynamic WPT system data. The results show the technical feasibility of such battery recharge technology by ensuring, on average, a state of charge of the forklifts is approximately constant. This work also gives an indication of the involved costs for the adoption of such technology in an industrial context and can constitute a reference study for future research in this field. After the current study about the performance of the system, the proposed work could be developed through several subsequent research projects. On the one hand, the authors will investigate the affordability of such technology in industrial contexts by carrying out an economic comparison with other battery recharging solutions, such as battery swapping systems and fast recharging systems. On the other hand, the application of the DWPT system has excellent potential in AGV applications since AGVs need fewer breaks than forklifts. It is possible to test if such a system can work continuously without stopping for recharges.

However, the proposed model can be further improved through different approaches. Firstly, as addressed above, the used model can only handle warehouses with orthogonal aisles. An improvement would be made by removing this constraint, although most warehouses have a plant layout with vertical and horizontal corridors [37]. A second improvement would be to parameterize the size of the WPT module and the edge length. These values are currently fixed under certain conditions (2.5 m for the DWPT module and 0.5 m for the edge length), and it is not straightforward to change them. A second future improvement of the presented work could be to analyze how the intermediate variables impact the final result, i.e., what are those variables between order arrival frequency, power, and efficiency of the WPT system, warehouse storage logic that most impact the distribution of coils and thus the total cost of the system. Finally, the last improvement would be to include the number of connected components in the cost function, e.g., by using the zeroth number of Betti in the solution graph. Keeping track of the gaps between components is extremely important, as digs need to be made on the floor. It would be more convenient and energy efficient to place the system as contiguous as possible. However, such a solution would make the model more complex to optimize.

Funding Open access funding provided by Politecnico di Torino within the CRUI-CARE Agreement.

Availability of data and materials Data supporting the findings of this study (forklift heat map of 60 simulations) are available from the corresponding author on request.

Code availability The code of the simulation model and of the optimization model are available from the corresponding author on request.

Declarations

Ethics approval Not applicable.

Consent to participate Not applicable.

Consent for publication Not applicable.

Competing interests The authors declare no competing interests.

References

1. European Commission (2011) A Roadmap for moving to a competitive low carbon economy in 2050. https://eur-lex.europa.eu/LexUriServ/LexUriServ.do?uri=COM:2011:0112:FIN:EN:PDF. Accessed 11 Oct 2022
2. Ferrero E, Alessandrini S, Balanzino A (2016) Impact of the electric vehicles on the air pollution from a highway. Appl Energy 169:450–459. https://doi.org/10.1016/j.apenergy.2016.01.098
3. Gould J, Golob TF (1998) Clean air forever? A longitudinal analysis of opinions about air pollution and electric vehicles. Transport Res D: Transport Environ 3:157–169. https://doi.org/10.1016/S1361-9209(97)00018-7
4. Sagaria S, Neto RC, Baptista P (2021) Modelling approach for assessing influential factors for EV energy performance. Sustain Energy Technol Assess 44:100984. https://doi.org/10.1016/j.seta.2020.100984
5. Renquist JV, Dickman B, Bradley TH (2012) Economic comparison of fuel cell powered forklifts to battery powered forklifts. Int J Hydrogen Energy 37:12054–12059. https://doi.org/10.1016/j.ijhydene.2012.06.070
6. Widrick RS, Nurre SG, Robbins MJ (2018) Optimal policies for the management of an electric vehicle battery swap station. Transp Sci 52:59–79. https://doi.org/10.1287/trsc.2016.0676
7. Unterreiner L, Jülch V, Reith S (2016) Recycling of battery technologies – ecological impact analysis using life cycle assessment (LCA). Energy Procedia. 99:229–234. https://doi.org/10.1016/j.egypro.2016.10.113
8. Cirimele V, Diana M, Freschi F, Mitolo M (2018) Inductive power transfer for automotive applications: state-of-the-art and future trends. IEEE Trans Ind Applicat 54:4069–4079. https://doi.org/10.1109/TIA.2018.2836098
9. Ruffo R, Cirimele V, Diana M, Khalilian M, Ganga AL, Guglielmi P (2018) Sensorless control of the charging process of a dynamic inductive power transfer system with an interleaved nine-phase boost converter. IEEE Trans Industr Electron 65:7630–7639. https://doi.org/10.1109/TIE.2018.2803719
10. Shi W, Dong J, Soeiro TB, Bauer P (2021) Integrated solution for electric vehicle and foreign object detection in the application of dynamic inductive power transfer. IEEE Trans Veh Technol 70:11365–11377. https://doi.org/10.1109/TVT.2021.3112278
11. Xia M, Aissa S (2015) On the efficiency of far-field wireless power transfer. IEEE Trans Signal Process 63:2835–2847. https://doi.org/10.1109/TSP.2015.2417497
12. Zhang Z, Pang H, Georgiadis A, Cecati C (2019) Wireless power transfer—an overview. IEEE Trans Ind Electron 66:1044–1058. https://doi.org/10.1109/TIE.2018.2835378
13. Covic GA, Boys JT (2013) Modern trends in inductive power transfer for transportation applications. IEEE J Emerg Selected Topics Power Electron 1:28–41. https://doi.org/10.1109/JESTPE.2013.2264473
14. Mi CC, Buja G, Choi SY, Rim CT (2016) Modern advances in wireless power transfer systems for roadway powered electric vehicles. IEEE Trans Industr Electron 63:6533–6545. https://doi.org/10.1109/TIE.2016.2574993
15. Cirimele V, Freschi F, Giaccone L, Pichon L, Repetto M (2017) Human exposure assessment in dynamic inductive power transfer for automotive applications. IEEE Trans Magn 53:1–4. https://doi.org/10.1109/TMAG.2017.2658955
16. Cirimele V, Diana M, Bellotti F, Berta R, Sayed NE, Kobeissi A, Guglielmi P, Ruffo R, Khalilian M, La Ganga A, Colussi J, Gloria AD (2020) The fabric ict platform for managing wireless dynamic

charging road lanes. IEEE Trans Veh Technol 69:2501–2512. https://doi.org/10.1109/TVT.2020.2968211
17. Laporte S, Coquery G, Deniau V, De Bernardinis A, Hautière N (2019) Dynamic wireless power transfer charging infrastructure for future evs: from experimental track to real circulated roads demonstrations. WEVJ. 10:84. https://doi.org/10.3390/wevj10040084
18. Tavakoli R, Pantic Z (2018) Analysis, Design, and demonstration of a 25-kW dynamic wireless charging system for roadway electric vehicles. IEEE J Emerg Selected Topics Power Electron 6:1378–1393. https://doi.org/10.1109/JESTPE.2017.2761763
19. Huang S-J, Lee T-S, Li W-H, Chen R-Y (2019) Modular on-road AGV wireless charging systems via interoperable power adjustment. IEEE Trans Industr Electron 66:5918–5928. https://doi.org/10.1109/TIE.2018.2873165
20. Zaheer A, Covic GA, Kacprzak D (2014) A bipolar pad in a 10-kHz 300-W distributed IPT system for AGV applications. IEEE Trans Industr Electron 61:3288–3301. https://doi.org/10.1109/TIE.2013.2281167
21. Faveto A, Traini E, Bruno G, Lombardi F (2021) Development of a key performance indicator framework for automated warehouse systems. IFAC-PapersOnLine. 54:116–121. https://doi.org/10.1016/j.ifacol.2021.08.013
22. Bartolini M, Bottani E, Grosse EH (2019) Green warehousing: systematic literature review and bibliometric analysis. J Clean Prod 226:242–258. https://doi.org/10.1016/j.jclepro.2019.04.055
23. Dotoli M, Epicoco N, Falagario M, Costantino N, Turchiano B (2015) An integrated approach for warehouse analysis and optimization: a case study. Comput Ind 70:56–69. https://doi.org/10.1016/j.compind.2014.12.004
24. Torabizadeh M, Yusof NM, Ma'aram A, Shaharoun AM (2020) Identifying sustainable warehouse management system indicators and proposing new weighting method. J Cleaner Product 248:119190. https://doi.org/10.1016/j.jclepro.2019.119190
25. Liu Z, Song Z (2017) Robust planning of dynamic wireless charging infrastructure for battery electric buses. Transport Res C: Emerg Technol 83:77–103. https://doi.org/10.1016/j.trc.2017.07.013
26. Helber S, Broihan J, Jang Y, Hecker P, Feuerle T (2018) Location planning for dynamic wireless charging systems for electric airport passenger buses. Energies 11:258. https://doi.org/10.3390/en11020258
27. Khan Z, Khan SM, Chowdhury M, Safro I, Ushijima-Mwesigwa H (2019) Wireless charging utility maximization and intersection control delay minimization framework for electric vehicles, Computer-Aided Civil and Infrastructure. Engineering 34:547–568. https://doi.org/10.1111/mice.12439
28. Sun X, Chen Z, Yin Y (2020) Integrated planning of static and dynamic charging infrastructure for electric vehicles. Transp Res Part D: Transp Environ 83:102331. https://doi.org/10.1016/j.trd.2020.102331
29. Kawakami T, Takata S (2012) Battery life cycle management for automatic guided vehicle systems. In: M. Matsumoto, Y. Umeda, K. Masui, S. Fukushige (Eds.) Design for innovative value towards a sustainable society. Dordrecht: Springer, pp. 403–408. https://doi.org/10.1007/978-94-007-3010-6_77
30. Matheys J, Timmermans JM, Mierlo JV, Meyer S, den Bossche PV (2009) Comparison of the environmental impact of five electric vehicle battery technologies using LCA. IJSM. 1:318. https://doi.org/10.1504/IJSM.2009.023977
31. Sullivan JL, Gaines L (2012) Status of life cycle inventories for batteries. Energy Convers Manage 58:134–148. https://doi.org/10.1016/j.enconman.2012.01.001
32. Janicak CA, Cekada TL (2016) Regulating forklift safety: strategies to prevent injury and improve compliance. Prof Saf 61:38–44
33. Dharmakeerthi CH, Mithulananthan N, Saha TK (2014) Impact of electric vehicle fast charging on power system voltage stability. Int J Electr Power Energy Syst 57:241–249. https://doi.org/10.1016/j.ijepes.2013.12.005
34. TMHE-Toyota Material Handling Europe, Technical specifications - Toyota Traigo 48, (2020). https://media.toyota-forklifts.eu/published/21449_Original%20document_toyota%20mh.pdf. Accessed 11 Oct 2022
35. VDI-Fachbereich Technische Logistik, VDI 2198 - Type sheets for industrial trucks, (2019). https://www.vdi.de/richtlinien/details/vdi-2198-typenblaetter-fuer-flurfoerderzeuge. Accessed 11 Oct 2022
36. Hart PE, Nilsson NJ, Raphael B (1968) A formal basis for the heuristic determination of minimum cost paths. IEEE Transact Syst Sci Cyber 4:100–107. https://doi.org/10.1109/TSSC.1968.300136
37. Pohl LM, Meller RD, Gue KR (2009) An analysis of dual-command operations in common warehouse designs. Transport Res E: Logistics Transport Rev 45:367–379. https://doi.org/10.1016/j.tre.2008.09.010